Effect of the number of sugar units on the interaction between diosgenyl saponin and membrane lipids

Joan Candice Ondevilla[a],[b] Shinya Hanashima[a,c]*, Akane Mukogawa[a], Darcy Garza Miyazato[a], Yuichi Umegawa[a,d], and Michio Murata[a,d,]*

[a]Department of Chemistry, Graduate School of Science, Osaka University, Toyonaka, Osaka 560-0043, Japan

[b]Department of Chemistry, De La Salle University, 2401 Taft Avenue, Manila 0922, Philippines

[c]Department of Chemistry and Biotechnology, Graduate School of Engineering, Tottori University, 4-101 Koyama-cho Minami, Tottori 680-8552, Japan

[d]Forefront Research Centre for Fundamental Science, Graduate School of Science, Osaka University, Toyonaka, Osaka 560-0043, Japan

ABSTRACT:

Saponin is the main bioactive component of the *Dioscorea* species, which are traditionally used for treating chronic diseases. An understanding of the interaction process of bioactive saponins with biomembranes provide insights into their development as therapeutic agents. The biological effects of saponins have been thought to be associated with membrane cholesterol (Chol). To shed light on the exact mechanisms of their interactions, we investigated the effects of diosgenyl saponins trillin (TRL) and dioscin (DSN) on the dynamic behavior of lipids and membrane properties in palmitoyloleolylphosphatidylcholine (POPC) bilayers using solid-state NMR and fluorescence spectroscopy. The membrane effects of diosgenin, a sapogenin of TRL and DSN, are similar to those of Chol, suggesting that diosgenin plays a major role in membrane binding and POPC chain ordering. The amphiphilicity of TRL and DSN enabled them to interact with POPC bilayers, regardless of Chol. In the presence of Chol, the sugar residues more prominently influenced the membrane-disrupting effects of saponins. The activity of DSN, which bears three sugar units, led to perturbation and further disruption of the membrane in the presence of Chol. However, TRL, which bears one sugar residue, increased the ordering of POPC chains while maintaining the integrity of the bilayer. This effect on the phospholipid bilayers is similar to that of cholesteryl glucoside. The influence of the number of sugars in saponin is discussed in more detail.

1. Introduction

Saponins are a general name given to compounds consisting of aglycones with sterol or triterpenoid structures and various sugar chains that are widely distributed in plants as secondary metabolites. They have historically contributed to human life through their beneficial effects [1,2]. Diosgenyl saponins, such as

trillin (TRL) and dioscin (DSN) (Fig. 1), which share the same sapogenin, diosgenin, are the main bioactive components of the *Dioscorea* species. These plants have been consumed for the treatment of illnesses, such as rheumatoid arthritis and bronchitis, and they have also been used for pain reduction and treatment of poor blood circulation [3]. Diosgenin, TRL, and DSN have distinct biological activities. The beneficial roles of diosgenin have been studied for the treatment of cancers, such as colon cancer and leukemia, for the management of diabetes and atherosclerosis, and for the prevention of neurodegenerative and metabolic disorders. Diosgenin is an industrially important precursor for producing hormones. TRL has also manifested pharmacological significance because of its antioxidant and anti-inflammatory effects [4][5]. DSN, one of the most potent membrane-active diosgenyl saponins, has anti-cancer, anti-inflammatory, hypocholesterolemia, and neuroprotective effects [6][7]. Diosgenyl saponins have been considered potential drug leads in the development of treatment strategies because of their wide spectrum of pharmacological and biological activities.

Diosgenyl saponins consist of a hydrophobic steroidal sapogenin and a hydrophilic sugar moiety, making them powerful amphiphiles with high surface activity. Thus, the biological effects of saponins have been attributed to their interaction with membrane lipids, as is the case with other saponin families. An intriguing behavior of saponins is their conspicuously characterized affinity for cholesterol (Chol) in membranes [8][9], which is considered to be related to their bioactivities. This highly recognized saponin–Chol interaction has been probed for its pharmacological relevance (e.g., treatment for hypercholesterolemia) and its effect on membrane phase behavior [8][10]. However, there have been reports of the activities of saponins on the membrane, even without Chol. The interaction of saponins with membranes is not necessarily Chol dependent but is likely influenced by their structure [11][12][13]. TRL and DSN, which differ in the number of sugars, have the same aglycon, diosgenin, which consists of a steroidal core and spiro-bicyclic side chain [14]. There have been a few reports on the relationship between the number of sugar units in saponins and biological activity. For example, Rh2, a type of ginsenoside with one glucose substitution at position 3, is more cytotoxic than Rg3, with two substitutions at position 3 [15].

Lipid–saponin interactions in membranes provide valuable insights into the pharmacokinetics because of the membrane penetration and cytotoxicity of these molecules [16,17]. Given that they are amphiphilic, these natural products can easily attach to lipid membranes and potentially modulate the membrane structure. We investigated TRL and DSN interactions with membrane lipids and evaluated their behavior in comparison with diosgenin [14], which is the sapogenin of TRL and DSN. Diosgenin lacks a sugar unit, TRL has one sugar, glucose, and DSN has three sugar units (Fig. 1). Thus, we elucidated the role of a sugar moiety in saponin in a more systematic manner. We also used diosgenin to correlate the steroidal backbone effect of saponins and to compare its saponin activities with that of Chol. Using different biophysical techniques, we revealed that the diosgenyl saponins have distinct membrane activity. For the majority of saponins, the key factor for their membranolytic activity is Chol, but diosgenyl saponins exert their bioactivities owing to their inherently strong affinity for phospholipids.

The competitive affinity of usual membrane lipids, such as phosphatidylcholine versus Chol, is often seen for membrane-active compounds other than saponins [18][19][20][21]. In these studies, solid-state NMR

has frequently been used to obtain the molecular basis for interaction between the compound and lipids/sterol in the atomistic level. We previously used ^{2}H and ^{31}P NMR to examine the short-lived interplay of membrane lipids with ^{2}H-labeled Chol and other sterol molecules [14][22][23][24][25].

In this study, we compared the interaction of saponin–Chol with that of saponin–diosgenin in membranes using biophysical methods, including solid-state NMR and fluorescence spectroscopy. Furthermore, the results underscored the degree of amphiphilicity of monodesmosidic saponins (i.e., the effect of the number of sugars as an indicator of membrane-permeabilizing capacity) [26] [27]. These results help clarify the effect of the sugar-chain size of saponin on Chol affinity and membrane activity in lipid bilayers.

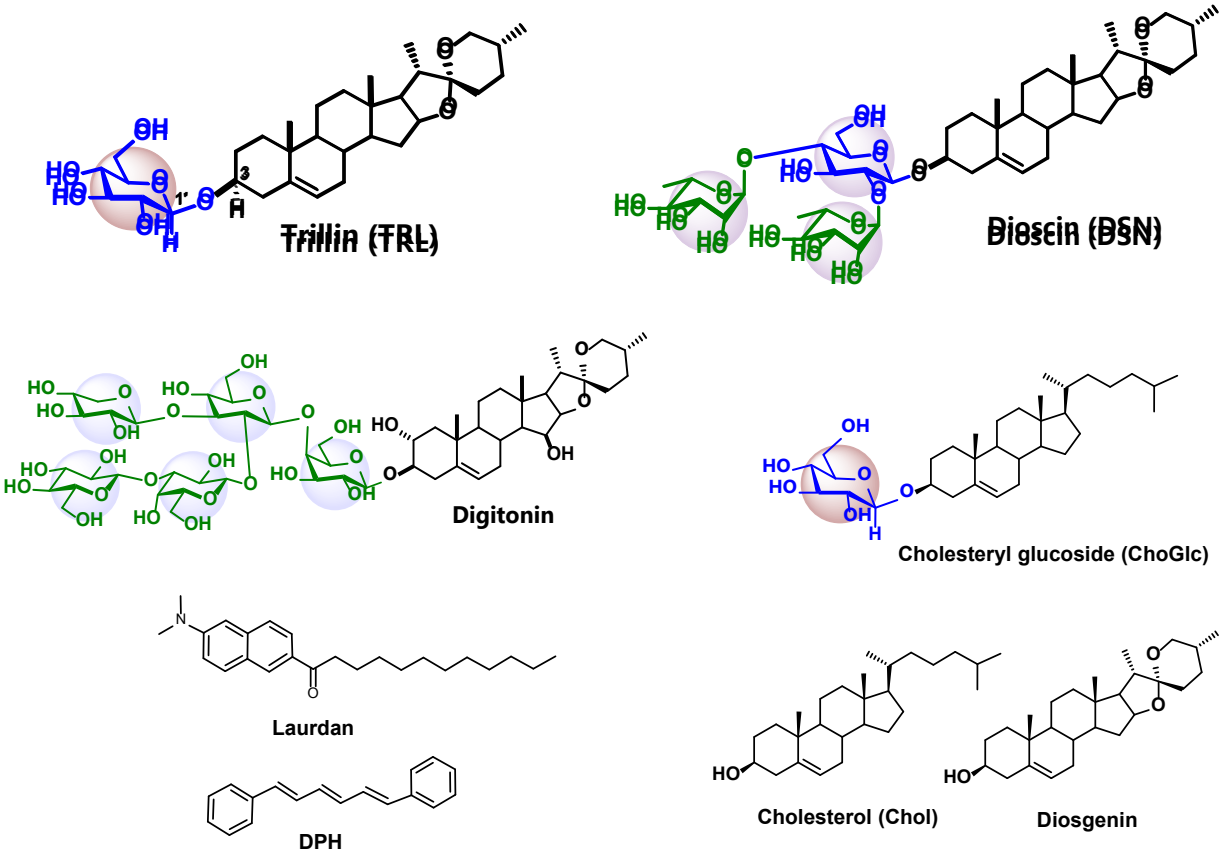

Figure 1. Structures of diosgenyl saponins bearing a diosgenin–sapogenin, digitonin, related compounds, and fluorescence probes used in this study. 3*d*-trillin (3*d*-TRL) and 1′*d*-trillin (1*d*-TRL) have one deuterium atom at the 3′ and 1′ positions (shown as "H"), respectively. Cholesteryl glucoside (ChoGlc) has a structure similar to TRL, except for the side chain.

2. Materials and Methods

2.1. Materials

Base lipids, such as 1-palmitoyl-2-oleoyl-sn-glycero-3-phosphocholine (POPC) and 1,2-dimyristoyl-sn-glycero-3-phosphocholine (DMPC) were purchased from NOF Corp., Japan (Coatsome®). Cholesterol and diosgenin were purchased from Nacalai Tesque Inc. and TCI Japan, respectively. Deuterated POPC

(10′,10′-d_2-POPC), in which two deuteron atoms were substituted at the 10′, 10′ position of a palmitoyl chain at the *sn*-1 position, was prepared by chemical synthesis as reported previously [14]. Diphenylhexatriene (DPH) and laurdan were obtained from Sigma-Aldrich. Laurdan was obtained from Cayman Chemicals. The deuterated sterols were synthesized based on previous protocols [14]. DSN was purchased from Carbosynth. Compton, Berkshire, United Kingdom. The deuterated TRLs, 3*d*-TRL and 1'*d*-TRL, were freshly synthesized, as described in Additional Materials and Methods section of Supporting Information. The positions of the deuterium-labels were confirmed by solution ^{1}H NMR spectra (Fig. S1). The solvents used were of spectroscopic grade, and all other chemicals used were of the highest available purity.

2.2. Preparation of liposomes

POPC or DMPC combined with different amounts of Chol or diosgenin were dissolved in $CHCl_3$/MeOH, mixed, and vortexed. The solvent was removed under an Ar stream and dried *in vacuo* overnight. The dried lipid mixture was then hydrated at 40°C for 1 h with Milli-Q for DSC experiments and 0.1 M PBS (pH 7.4) for fluorescence measurements and subsequently subjected to five freeze–thaw cycles. Multi-lamellar vesicles (MLVs) were used immediately after preparation. For fluorescence measurements, the MLVs were further sonicated (SND Co. Ltd. Japan 100 W) for 10 min to produce unilamellar vesicles [28]. For solid-state NMR measurements, saponin, lipid mixtures containing POPC, and/or sterol with deuterated lipids, 3*d*-Chol, 3*d*-diosgenin, or 10′,10′-d_2-POPC were prepared in organic solvents ($CHCl_3$ and MeOH), vortexed, and dried in Ar. The dried lipid film was then hydrated with Milli-Q water for 30 min. The samples were then freeze-thawed (five cycles) and lyophilized. The dry lipid was hydrated with an equal amount of deuterium-depleted water. To completely homogenize the sample, we performed 10 freeze–thaw–centrifuge cycles. The samples were then transferred carefully to an insert (Bruker BL4 HR-MAS Kel-F) [14].

2.3. Differential scanning calorimetry (DSC) measurements

DSC was measured using Nano-DSC (TA Instruments; New Castle, DE, USA). Approximately 3 mM of the lipid sample was injected into the DSC sample cell. Heating–cooling scans were performed between 10°C and 50°C with a linear temperature gradient of 0.5°C/min. Thermograms were analyzed using NanoAnalyze (TA Instruments).

2. 4. Hemolysis assay

Human blood samples were collected on the day of the experiment. The samples were washed with 10 mM PBS at pH 7.4 and mixed using a vortex mixer. The solution was centrifuged for 5 min at 2,000 rpm, and the supernatant was carefully discarded. The pellet was resuspended in PBS and labeled as a 10% (v/v) red blood cell (RBC) solution. The 10% RBC was divided into three portions. The first portion was mixed with PBS to obtain a 1% non-depleted RBC solution. The second portion was incubated with 3.5 mM methyl-

β-cyclodextrin (MβCD) at 37°C for 2 h, followed by centrifugation and resuspension in PBS to obtain a Chol-depleted RBC 1% (v/v) solution. The last portion was treated similarly to the second portion, but the cells were treated with a 7:1 mole ratio of Chol/MβCD at 37°C for 2 h to restore Chol in the cell membrane. The samples were centrifuged and resuspended in PBS to obtain a 1% (v/v) Chol-repleted solution.

The cells were seeded into a 96-well microplate, and saponins were added to the assigned wells, followed by mixing at a moderate speed. The samples were incubated for 18 h at 37°C, followed by centrifugation at 2,000 rpm for 5 min. The absorbance of the supernatant was measured at 450 nm using a microplate reader (Corona Electric). A mixture of milliQ water/10% RBC (v/v; 9:1 volume ratio) was used as a positive control, and 1% (v/v) RBC/PBS (18:1 volume ratio) was used as the blank. Triplicate samples were prepared for each saponin concentration. Hemolysis was calculated as follows:

$$\%\ \text{Hemolysis} = \frac{A_{sample} - A_{blank}}{A_{positive\ control}} \times 100$$

2.5. Calcein leakage assays

The ability of saponins to induce leakage in large unilamellar vesicles (LUVs) was determined by measuring the intensity of calcein. Similarly, time-dependent calcein leakage was examined with calcein-loaded LUVs. LUVs were prepared using POPC and various sterols. Pure POPC and 9:1 POPC/Chol were dissolved in chloroform in a round-bottom flask. The solvents were removed and dried under reduced pressure at 35°C and further dried overnight *in vacuo*. The lipid film was resuspended in 60 mM calcein (1 mL) in 10 mM Tris–HCl buffer containing 150 mM NaCl and 1 mM EDTA at pH 7.4 and mixed using a vortex mixer for 1 min. Five cycles of freezing (−20°C) and thawing (65°C) were performed to produce MLVs. The MLVs were subjected to extrusion using a LiposoFast Basic extruder (pore size, 200 nm, Avestin Inc., Ottawa, Canada) 19 times to obtain homogeneous LUVs. Excess calcein was removed using a Sepharose 4B column (GE Healthcare, Uppsala, Sweden). The lipid and Chol concentrations of the LUV fraction were quantified using the phospholipid C test and the cholesterol E test kits, respectively. The final concentrations of the phospholipid and Chol in the resulting LUVs were adjusted depending on the measurements to be conducted. LUVs were immediately used for measurement to prevent premature vesicle leakage. A 96-well Nunclon Delta Surface (black) F-bottom microplate (Thermo Scientific, Waltham, MA, USA) was used, and the initial fluorescence was measured using an MTP-800 series, Corona Electric Multimode Microplate Reader (Ibaraki, Japan) at an excitation wavelength of 490 nm and an emission wavelength of 517 nm. Saponins were added to the LUVs, which were mixed at a slow speed for 1 min and allowed to stand at room temperature for 5 min, 30 min, 1 h, and 2 h prior to fluorescent measurement after saponin-induced leakage. Triton-X (10%) was added to the mixture to obtain a condition of 100% leakage. In the time-course calcein leakage assays, the measurements were carried out using a Jasco FP-6500 fluorescence spectrofluorometer (Tokyo, Japan). The sample was continuously mixed using a magnetic stirrer, and fluorescence was stabilized for 2 min. Saponin was added, and fluorescence changes were

observed for a total of 5 min. Triton-X was then added for the 100% leakage condition. The % calcein leakage was calculated using the following equation:

$$\% \text{ Calcein leakage} = \frac{I_S - I_0}{I_T - I_0} \times 100$$

where I_S, I_T, and I_0 are the fluorescence intensities after saponin addition, at 100% LUV leakage, and background, respectively [29].

2.6. Fluorescence measurements

Solutions (100 μM each) of laurdan and DPH were prepared in EtOH. Liposomes in PBS buffer (3 mL, the concentration of total lipids was 50 μM) were incubated with the probes (lipid:probe ratio of 200:1) at 37°C for 3 h. For laurdan, steady-state fluorescence emissions from 400 nm to 600 nm were recorded using an FP-8500 spectrofluorometer (JASCO, Tokyo, Japan) with an excitation wavelength of 340 nm and an emission wavelength from 400 nm to 600 nm. Generalized polarization (GP_{ex}) was calculated from the emission intensities at 440 (I_{440}) and 490 (I_{490}) nm using the following equation adapted from Parasassi et al. [30]:

$$GP_{ex} = \frac{I_{440} - I_{490}}{I_{440} + I_{490}} \quad (1)$$

The DPH anisotropy measurements were performed using an FP-8500 spectrofluorometer (JASCO, Tokyo, Japan) working in the L-format and equipped with automatic polarizers. The samples were excited at λ_{ex} = 358 nm, and the fluorescence intensity was monitored at λ_{em} = 430 nm. Steady-state anisotropy (r) was calculated using the following equation:

$$r = \frac{I_{vv} - GI_{vh}}{I_{vv} + 2GI_{vh}} \quad (2)$$

where I is the fluorescence intensity, and the v and h subscripts denote the vertical and horizontal settings of the excitation and emission polarizers, respectively. G is an instrumental correction factor and was calculated individually for each sample according to the equation: $G = I_{hh}/I_{hv}$

2.7. ^{2}H and ^{31}P solid-state NMR

Solid-state ^{31}P and ^{2}H-NMR spectra were recorded on a Bruker AVANCE400 spectrometer at 400 MHz for ^{1}H frequency. For ^{2}H-NMR, a 5 mm ^{2}H static probe using a quadrupolar echo sequence was used. The 90° pulse width was 5 μs, the inter-pulse delay was 30 μs, the echo delay was 24 μs, and the repetition delay was 0.5 s. The sweep width was 250 kHz, covered with 4,096 points, and the number of scans ranged from 150,000 to 200,000. The probe temperature was set at 30 °C.

For ^{31}P NMR, a 4 mm HXY triple-resonance MAS probe using direct excitation (without MAS) was used. The 90° pulse width was 4.35 μs with a relaxation delay of 2 s. ^{1}H decoupling was performed with the Spinal-64 sequence at 30 kHz. The sweep width was 64 kHz, covered with 4,096 points, and the number of scans ranged from 4,000 to 5,000. The probe temperature was set to 30 °C. The chemical shift anisotropy (CSA) is expressed as $\delta_{//} - \delta\perp$ in the text.

3. Results

3.1. Hemolysis and calcein leakage assays

Hemolysis and calcein-leakage assays are standard methods for identifying membrane-permeabilizing agents. In a hemolysis assay, DSN induced a complete lysis of RBCs comparable to the hemolytic activity of digitonin, a well-known membrane disrupting saponin [31]. This result is consistent with a previous report showing that DSN has potent hemolytic activity and cytotoxicity toward cultured cells [32]. By contrast, TRL was virtually inactive (Fig. 2).

We evaluated the membrane-permeabilizing activity of TRL and DSN using a calcein leakage assay according to the conditions used in previous saponin studies (Fig. 3) [31][11]. In this experiment, we evaluated lipid membrane disruption using model membranes containing no proteins. In POPC-Chol bilayers (Fig. 3B), we observed a similar trend to that of the hemolysis assay. In the Chol-containing bilayers, DSN induced calcein leakage for 5 min more efficiently than did TRL, while in POPC unitary bilayers DSN and TRL showed similar weak activity. The results of the calcein-leakage for long incubation times are shown in Fig. S2. The leakage activity of the TLR-incubated group was relatively elevated at 30-min or longer incubation, which could be attributed to the domain formation of bilayers by saponin. Since the main purpose of this study was to examine the direct effect of saponin inserted into bilayers, we focused on a relatively short incubation time of 5 min to suppress the effect of domain formation [31].

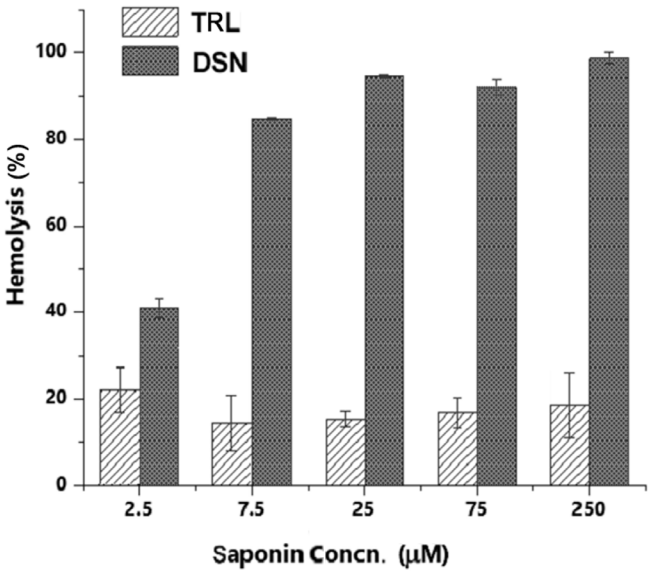

Figure 2. Hemolytic activity (%) of TRL (hatched) and DSN (gray). The error bars denote the SEM derived from triplicate experiments. Hemolytic activity (%) of TRL (hatched) and DSN (gray) on red blood cells. The control percentage was around zero with a SEM value similar to that of the TRL results.

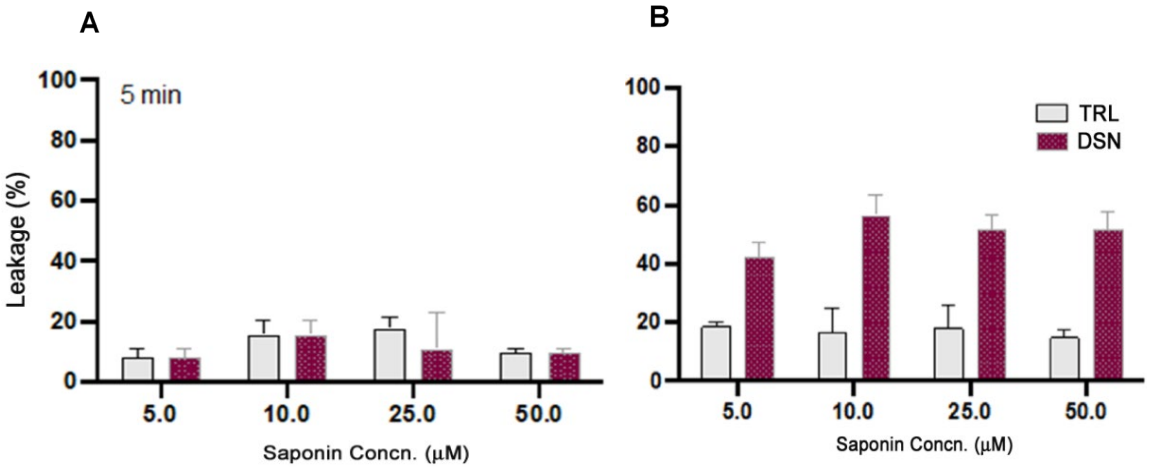

Figure 3. Calcein leakage from LUVs consisting of POPC (**A**) and POPC: Chol (9:1) (**B**) induced by TRL (light gray) and DSN (maroon) for 5 min at different concentrations. The % leakage values for the control without TRL and DSN were very close to those for TRL at 5.0 μmol/L for both lipid compositions. The error bars denote the SEM derived from the triplicate experiments. The leakage data for longer incubation times are presented in Fig. S2.

3.2. Differential scanning calorimetry

The effects of saponins on the thermotropic behavior of DMPC membranes were evaluated using DSC. The phase transition temperature of POPC is -3 ºC, which means that antifreeze must be used to perform DSC experiments, which would not reproduce the binding of saponin to the membrane in the calcein and hemolysis experiments. Instead, we used DMPC, which has a phase transition temperature near room temperature. The MLVs were prepared, and the endothermic profiles of DMPC and DMPC/Chol bilayers were examined after incubation with 50 μM saponins (Fig. 4). The TRL-incubated MLVs (Fig. 4, middle panel II) showed almost identical endothermic profiles to the non-incubated MLVs, except for the peak widths. The integrity of the vesicles was mostly maintained. The cooperativity of the acyl chains of DMPC was slightly decreased by TRL, as demonstrated by the broadening of the peaks. By contrast, the MLVs treated with DSN at different Chol contents (Fig. 4 III) revealed notable differences. The thermogram of the DMPC bilayers without Chol (Fig. 4A, III) gave rise to a broader shoulder right below the main transition temperature, which suggested the disordering of the phospholipids' gel domain caused by DSN. This endothermic peak appeared in the presence of Chol (Fig. 4B/C, III). This observation suggests the formation of domains rich in DSN complexed with DMPC and/or Chol. A similar tendency was observed for DMPC incorporated with diosgenin (Figure S3).

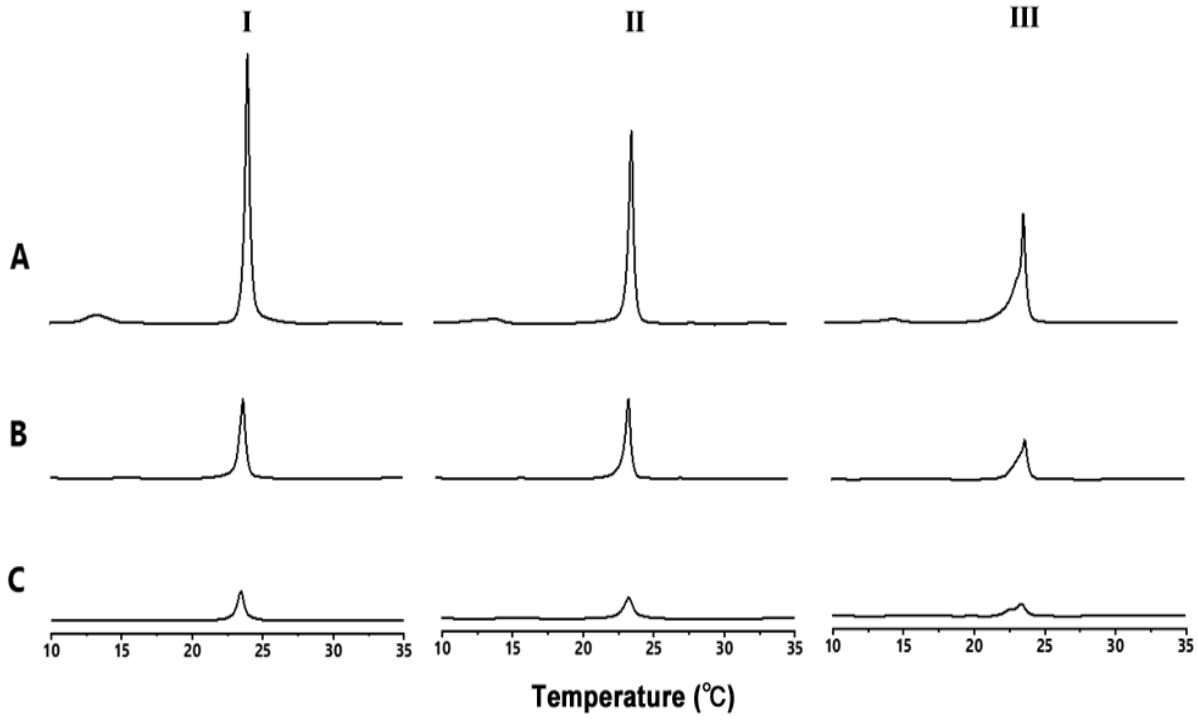

Figure 4. DSC thermograms of unitary DMPC MLVs (**A**), DMPC with 5 mol% Chol (**B**), and DMPC with 10 mol% Chol (**C**) upon incubation without saponin (I) and with 50 μM TRL (II) and 50 μM DSN (III). The lipid concentration was 3 mM.

3.3. Water penetration into bilayers and bilayer ordering evaluated by laurdan and DPH

Laurdan is a suitable probe for monitoring the hydration state and the acyl chain order at the interfacial depth of the membrane, while DPH can monitor the acyl chain order deeper in the membrane. Acyl chain order reflects membrane stiffness. The solvatochromic properties of laurdan were exploited in membrane studies to examine membrane polarity and hydration states. The parameter GP_{340} provides reasonable estimates of the overall lipid environment. A vital characteristic assessed by Laurdan GP_{340} is the presence of water penetration into a lipid bilayer [33]; however, GP_{340} values can also be used to check the fluidity and order of the membrane [34]. The LUVs were incubated at 37°C with different concentrations of the saponins. The GP_{340} values for TRL-treated LUVs increased for unitary POPC and Chol- or diosgenin-incorporated POPC (Figs. 5 and S4). For the DSN-treated LUVs, the GP_{340} values for POPC LUVs increased, indicating an increase in the rigidity of the membrane. However, in the presence of Chol (Fig. 5B) or diosgenin (Fig. S4), the addition of DSN and digitonin resulted in a more polar membrane environment because of membrane disruption by the saponins at higher contents. In the absence of Chol or diosgenin, both TRL and DSN exerted increases in bilayer ordering, whereas the effect of TRL was more prominent even at the highest concentration.

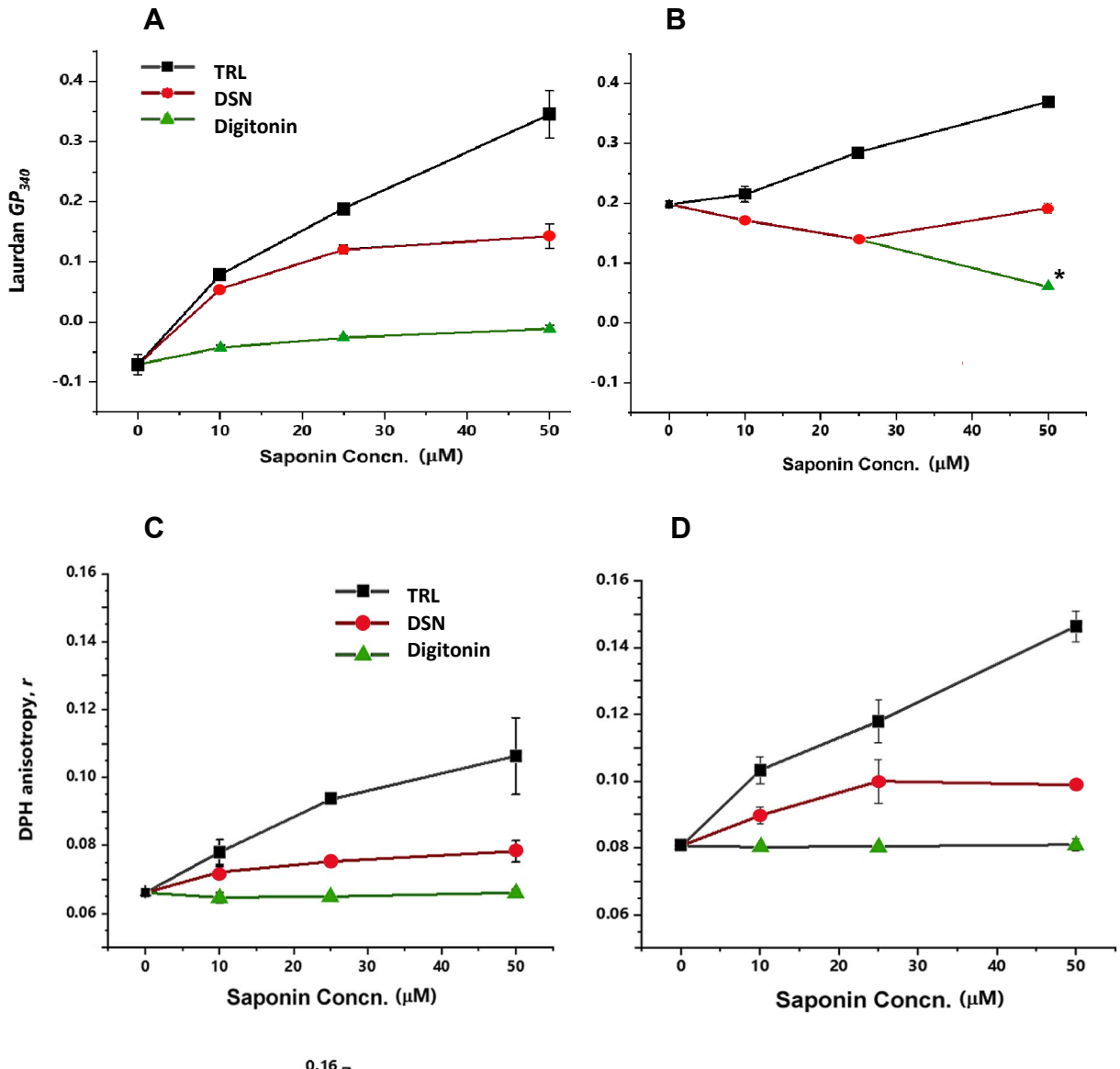

Figure 5. Membrane hydration and order estimated by Laurdan GP_{340} values of POPC (**A**) and POPC-Chol 9:1 (**B**), and by fluorescent anisotropy (*r*) of the DPH of POPC (**C**) and POPC-Chol 9:1 (**D**) at 37°C with TRL (black line with square symbols), DSN (red line with circle symbols), and digitonin (green line with triangle symbols) at 5, 10, 25, and 50 μM, which were added to the LUVs (50 μM) containing 1 mol% laurdan. *MLVs were disrupted under 50 μM digitonin.

The results of the DPH anisotropy verified the Laurdan GP_{340} data. The insertion of TRL into the membrane caused the membrane to be more packed, as depicted by the significant increase in the anisotropy of DPH, even in the presence of Chol (Fig. 5D). DSN also had the same propensity in pure POPC membranes. However, at higher concentrations, the increase in DPH anisotropy was slow and steady. With Chol or diosgenin, the anisotropy values tapered off at higher concentrations of DSN, indicating an increase in the fluidity of the membranes (Fig. 5D). The interaction between Chol and DSN was assumed to create curvature strain, and the major structural consequence was the disordering of the acyl chains of POPC. This effect by DSN and digitonin was confirmed by the GP_{340} results in Fig. 5B, where digitonin at 50 μM damaged membrane integrity, causing the penetration of water into the bilayer interior. The lack of change in the DPH anisotropy of Chol-free membranes with digitonin was due to the very small amount of digitonin bound to the membrane (a similar trend was observed for the GP_{340} values). The reason that the anisotropy of Chol-containing membranes was not much changed by digitonin was probably because little DPH was distributed to the domains where digitonin and Chol localized.

3.4 ^{2}H and ^{31}P solid-state NMR spectra of saponin-containing POPC membranes using ^{2}H lipid probes

To determine the orientation and dynamics of the saponins in lipid bilayers and their interaction with sterols, we used three types of deuterated probes: 3*d*-Chol and 3*d*-diosgenin as sterol probes, 1'*d*-TRL and 3*d*-TRL as saponin probes, and 10′,10′d_2-POPC as a phospholipid probe. These deuterium probes reproduce the order and orientation of the original compound, which can be evaluated by their quadrupolar splitting widths. Among these probes, the NMR spectra of 3*d*-Chol and *3d*-diosgenin are shown in Fig. 6. The $\Delta\nu$ values of the two probes in the presence of TRL or DSN were very close (Table 1), suggesting a similarity in saponin's interactions with diosgenin and with Chol in POPC bilayers. The smaller $\Delta\nu$ values of 3*d*-Chol and 3*d*-diosgenin in the presence of 10 mol% DSN revealed that the ordering and/or orientation of Chol and diosgenin were susceptible to the membrane-perturbing effect of DSN.

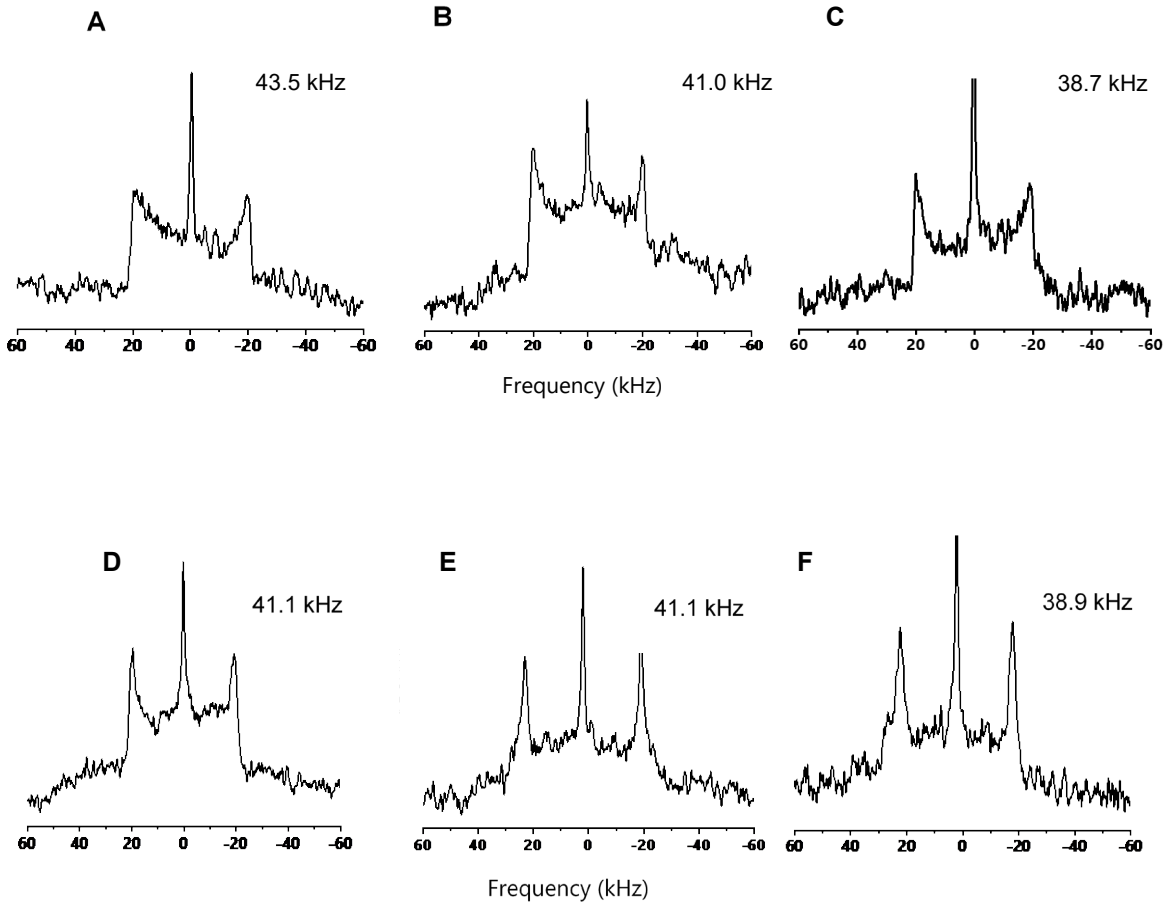

Figure 6. ^{2}H NMR spectra of 3-*d*-Chol (10 mol%) in panels **A**-**C** and 3-*d*-diosgenin (10 mol%) in panels **D**-**F** in POPC bilayers in the absence of saponins (**A**, **D**), in the presence of 10 mol% TRL (**B**, **E**), and in the presence of 10 mol% DSN (**C**, **F**). The spectra were measured at 30°C. The central peak in each spectrum may be due to residual deuterated water.

To obtain a clearer picture of the membrane effects of the diosgenyl saponins, we adopted 10′,10′-d_2-POPC. Given that this position of PC is known to be sensitive to the Chol-induced ordering effect on the acyl chains [35][24], we examined saponin's effects on acyl chain ordering and the packing of POPC. The bilayers containing 10 mol% TRL resulted in an increase in the quadrupolar splitting value ($\Delta\nu$) of 23 kHz, although this was slightly lower than the $\Delta\nu$ value (25 kHz) in the POPC–Chol bilayers (Table 1). This result was consistent with the fluorescence spectroscopy data, which revealed that TRL intercalated in unitary POPC membranes and consequently increased the packing of POPC acyl chains. DSN incorporation also minimally increased $\Delta\nu$, denoting a decrease in the membrane fluidity of POPC, as described in the fluorescence spectroscopy results. This significant reduction in $\Delta\nu$ was observed with digitonin in the POPC–Chol membrane, which could be a result of perturbation of the membrane integrity by digitonin. Contrary to DSN or TRL, we speculated that digitonin could not efficiently bind to unitary POPC bilayers, probably due to its large sugar moiety, which resulted in an unchanged $\Delta\nu$ value of 10′,10′-d_2-POPC (Table 1). A previous

study has reported that digitonin hardly binds to SOPC (stearoyl-oleoyl-PC) bilayers, which are similar to those of POPC [26].

For POPC membranes with Chol, TRL intercalation resulted in a marked increase in the $\Delta\nu$ of 10′,10′-d_2-POPC, whereas DSN and digitonin incorporation decreased $\Delta\nu$. The incorporation of TRL, aligned in an upright fashion, in POPC membranes with Chol caused an increased order in the system and made the membranes more rigid. This transformation was also observed with the *3d*-Chol probe, in which the realignment of the sterol probe was affected by the presence of TRL. In the case of DSN, the lower $\Delta\nu$ indicated curvature changes as DSN was incorporated into the system. By contrast, for digitonin, the $\Delta\nu$ decreased and approached the value for a pure POPC membrane. A careful interpretation of this result can be derived from the abstraction of Chol from the membrane, as the sterol associates with digitonin.

We simultaneously recorded ^{31}P NMR spectra using the same membrane preparations to examine the integrity of the bilayer structure of POPC (Table 1 and Fig. S5). TRL appeared to maintain the integrity of the bilayer structure of POPC in the presence or absence of Chol. DSN slightly disrupted the bilayer structure in the presence of sterols, but the disruption was minor compared to that of digitonin; in the POPC-Cho bilayer, a small anisotropic peak appeared for the DSN spectrum (Figure S4D), suggesting a local increase in bilayer curvature (see Discussion for a detailed interpretation of the ^{31}P NMR results).

3.5 ^{2}H NMR study of saponin behavior in bilayers using 3d-TRL and 1'd-TRL

TRL was also labeled to explore the orientation of the saponins in the membrane. The TRL was labeled at the C3 position of the aglycone (3*d*-TRL) and at the C1' of the sugar moiety (1'*d*-TRL) (Fig. 1). These two site-specific probes were separately used in POPC membranes with and without Chol. Fig. 7 shows the ^{2}H NMR spectra of the POPC MLVs with 10 mol% of the saponin probe, with the spectra on the right being that of POPC-Chol (9:1). The spectra revealed a typical Pake doublet, implying that the parallel orientation of the saponin to the membrane was normal. This observation verified the permeation of TRL in POPC vesicles, as suggested by the fluorescence spectroscopy data. In the presence of Chol, the $\Delta\nu$ value increased (Fig. 7) for both *d*-TRL and 1'*d*-TRL probes, implying that the saponin reoriented itself with Chol in the membrane. This is an indication that TRL was associated with Chol and that this interaction caused the membrane to be more ordered.

We recently reported the results of solid-state NMR on the behavior of cholesteryl glucoside (ChoGlc in Fig. 1) in bilayers [36]. The effect of a sugar unit on the ordering of acyl chains was investigated by assessing the magnitude of the $\Delta\nu$ value for 10′,10′-d_2-POPC, which was 91% that of Chol, whereas TRL was almost equivalent to diosgenin (Table 1). In addition, the ordering of the TRL itself at the 3*d* position was compared with that of ChoGlc, and they were very close; in the POPC membrane, the TRL was 39.5 kHz, whereas the ChoGlc was 40.4 kHz [36].

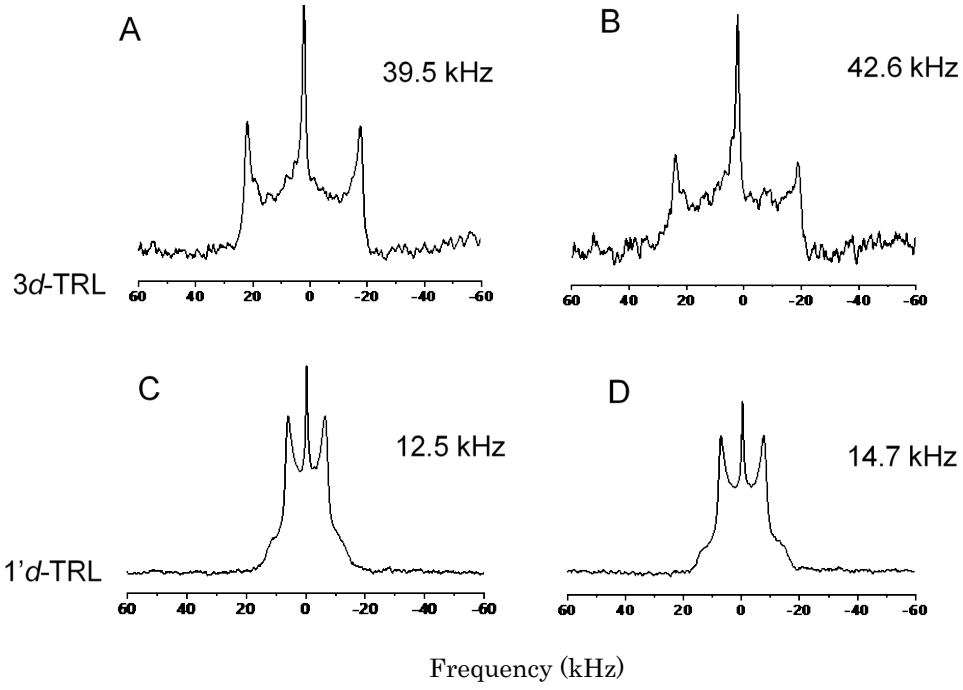

Figure 7. Solid-state ^{2}H NMR spectra of 10 mol% deuterated TRLs in POPC and POPC–Chol (9:1) systems. **A** and **B**: 3*d*-TRL (Fig. 1) in the POPC and in POPC–Chol (9:1) bilayers, respectively. **C** and **D**: 1'*d*-TRL (Fig. 1) in the POPC and POPC–Chol 9:1 bilayers, respectively. The Δν values are shown in each spectrum. The central peak in each spectrum may be due to residual deuterated water.

4. Discussion

Diosgenyl saponins, such as DSN and TRL, possess multiple pharmacological effects; for example., the saponin extract has been subjected to a US clinical trial for treating diabetic neuropathy [37]. However, the mechanism in saponin–membrane interactions, which are a fundamental assessment of the drug's activity, has not been thoroughly explored for these saponins. A generally accepted notion about saponin–membrane interplay is their intrinsic affinity for Chol. However, the molecular mechanism of saponin–sterol interactions and their membrane-disrupting activity are not fully understood for this saponin class. To compare the behavior of DSN and TRL with a well-investigated saponin, we adopted digitonin as a reference compound. Additionally, to clarify the difference between saponin–Chol and saponin–saponin affinity in the bilayer interior, we examined the influence of diosgenin, the sapogenin of TRL and DSN, on saponin-induced membrane effects and compared it with those of Chol.

Here, it is important to summarize the interactions of the diosgenyl saponins with the membrane lipids obtained from the present results. Notably, the membrane ordering or disordering effects of saponin seem inconsistent across the experiments; DPH anisotropy in the Chol-containing membrane was significantly increased by the addition of DSN up to 25 μM (Fig. 5D), which meant that the acyl chain order was enhanced. By contrast, the ^{2}H NMR results showed a slight decrease in the acyl chain order (Table 1, the difference was -2 kHz) due to the interaction with DSN. We speculate that the difference in the preparation method is at least partially responsible for the discrepancy in the experimental results. In the fluorescence experiments with laurdan and DPH, saponin was added to the preformed vesicles, whereas in the NMR experiments saponin was mixed at the beginning of the vesicles preparation. Interactions of lipids with DSN reduce the fluctuations of the acyl chains, while the relatively high affinity of DSN for POPC-Chol bilayers led to a broader distribution of acyl chain orientations (Figure 8D). Under the NMR conditions, saponin was evenly distributed in both leaflets with little strain between outer and inner leaflets. Therefore, the distortion of the bilayer in the presence of saponin induces local membrane undulation. The orientation changes caused by lipid diffusion during the long NMR acquisition time led to a decrease in the ^{2}H-splitting width. However, in the DPH experiment, saponin mostly bound to the outer leaflet of the vesicle bilayers, inducing a curvature change over relatively large areas. Thus, lipid diffusion hardly caused a decrease in DPH anisotropy during the short time scale of the anisotropy measurement. Therefore, we believe that the observed increase in DPH anisotropy was largely due to the stronger interaction of saponin with lipids and DPH, which resulted in a decrease in the wobbling of the acyl chains and DPH.

We estimated how much difference in the membrane concentration of saponin would occur between the two methods with different additions of saponin. Given that the ^{2}H NMR spectra of 10 mol% TRL in Fig. 7A/B showed a characteristic spectral width for molecules bound perpendicularly to the membrane, TRLs must have been mostly inserted in the bilayer. Having devised a method to estimate the membrane partition efficiency from DPH anisotropy [42], we attempted to calculate the partition of 10 μM TRLs and DSN to the POPC-based bilayers. We roughly estimated that 10 – 40 mol% of saponin per lipid was bound to the membrane under the conditions of the calcein, laurdan, and DPH experiments, which were comparable with

the saponin content in bilayers in previous studies [12][31]. Considering these results, the differences in membrane concentrations of saponin between NMR measurements and hemolysis/leakage/ fluorescence experiments are not considered extreme.

Next, we examined the effects of diosgenin, which is the sapogenin of TRL and DSN and lacks a sugar chain. Diosgenin in bilayer membranes tends to increase the order of lipid acyl chains, which should be due to the interaction between the steroidal core and the acyl chains [14]. TRL significantly increased the order of the acyl chains (10′,10′d_2-POPC in Table 1) and DSN also slightly raised the order of the lipid chains (Fig. 5). A small but significant difference in the $\Delta\nu$ values between Chol and diosgenin (or TRL, Table 1) should be due to a difference in the side chain structure of Chol and diosgenin since the side chains have a significant effect on the order effect of lipid acyl chains [38][39].

A comparison of the NMR parameters of diosgenin, TRL, and DSN based on the order of the sugar chain size revealed interesting features, as summarized in Table 1. Judging from the reduction of ^{2}H splitting width of 3*d*-Chol with increasing the number of saponin sugar units (the top row of Table 1), the orientation and ordering of Chol were greatly influenced by interaction with saponin, probably due to the depth position of Chol and the lipid-chain packing around Chol. This effect of saponin was less effective for diosgenin (2nd row of Table 1). TRL was inserted in bilayers as shown in the ^{2}H NMR experiment for 3*d*-TRL (Fig. 7), where a reasonable $\Delta\nu$ value for a vertically oriented sterol core was observed. We performed detailed ^{2}H NMR experiments on ChoGlc and estimated its orientation by MD calculation [36]. Assuming the same order parameter (S_{mol}) for TRL and ChoGlc, the orientation angle of TRL (as the angle between the C3-C17 long molecular axis and the membrane normal) and that of the ChoGlc sterol core were estimated to be similar; the orientation of TRL to the bilayer normal is 10 –20°. Moreover, as described in Section 3.4, the similarity of TRL to ChoGlc in preserving bilayer integrity implies that the sterol core of TRL stayed at a depth similar to that of ChoGlc, which was close to the depth position of Chol in bilayers [36]. This position of the TRL's sapogenin efficiently enhances the ordering of the acyl chains and helps maintain the planar bilayer structure.

These results indicate that the depth position of the saponin along the bilayer normal depends on the number of sugars; diosgenin largely stays at the same depth as Chol, the diosgenin sapogenin of TRL may reside at similar (or slightly shallower) depth such that its glucose moiety comes close to the phosphodiester of POPC (this may cause the higher CSA value of POPC), and the DSN sapogenin possibly resides at an even higher position and lifts the membrane lipids to induce the curvature change of bilayers. The ^{31}P CSA of POPC in the presence of DSN bearing three sugar units showed a greater increase in the average curvature in the Chol-containing bilayers than in the diosgenin-containing bilayers (6th and 7th rows of Table 1 and Fig. S4). The GUV image in Fig. S9 also suggests an increase in the curvature of the Chol-containing bilayer due to DSN.-This result suggests that the sapogenin moiety of DSN interacts with Chol with a higher affinity over sapogenin itself (diosgenin) in the bilayer interior. The presence of an oxygen-containing spiro-bicycle may interfere with the homophilic interaction of diosgenin with the sapogenin of DSN (or TRL) in the hydrophobic bilayer interior. Additionally, the iso-octyl side chain of Chol has a strong ordering effect in a bilayer environment [40], which further enhances the VDW contact between Chol and saponin. Even in the

absence of Chol, however, DSN showed some affinity for POPC unitary bilayers (Fig. 5). The presence of Chol enhanced the affinity of DSN to bilayers (Fig. 5) but to a lesser extent than that of digitonin (e.g., Table S1). DSN changed the curvature and destabilized the chain packing of POPC-based bilayers to a certain extent, whereas TRL did not show such effects. This effect of DSN was considerably weaker than that of digitonin, probably leading to its weaker ability in micelle formation [26].

Based on these findings, we inferred a molecular mechanism for the membrane-permeabilizing activity of diosgenyl saponins as shown in Fig. 8. Diosgenyl saponins, represented by DSN, interact with both Chol and phospholipids in membranes to modulate the bilayer structure. The detergent effect of DSN, which has three sugar units, was apparently weaker than that of digitonin [29], which has five sugar units. This may be because the hydrophilicity of DSN, corresponding to its ability to extract Chol/lipids in the bilayer into the aqueous phase, is lower than that of digitonin. Regarding the number of sugar units within diosgenyl saponins, DSN had a much stronger membrane disrupting effect than TRL, possibly because the sugar units of DSN branch off from the sugar directly bound to the sapogenin and were more exposed to the aqueous phase. The single sugar unit of TRL made the cross-sectional area of the bilayer–water interface region comparable to that of sapogenin, whereas the three sugars of DSN at the boundary region made the cross-section area much larger than that of TRL, thus enhancing the membrane-disrupting activity (Fig. 8) [42]. DSN interacts not only with Chol but also with phospholipids in the membrane to modulate the bilayer structure and curvature. In the presence of DSN, ^{31}P CSA was markedly reduced compared to TRL (Table 1), which implies that DSC induces a curvature rise of POPC/Chol membranes. Confocal images of GUVs [43] also showed a curvature rise and budding of the bilayers (Fig. S6). Thus, unlike digitonin, DSN does not form a rigid Chol-enriched domain (complex) structure.

Further, some DSN molecules that did not insert deeply into the bilayer interior probably covered the surface of the membranes (not shown in Fig. 8). Even in this case, DSN may partly disrupt bilayer stability and increase membrane permeability (e.g., the Carpet model). We previously found a similar effect with ginsenoside Rh2 [44].

Digitonin behaves in a different modality than DSN. As described earlier, its strong amphiphilicity efficiently disrupts membrane integrity. The less hydrophobic sapogenin bearing five sugar units destabilized the lipid packing and further induced water penetration into the membrane interior. Under these circumstances, a “saponin–Chol complex” is generated in the membrane, allowing digitonin to extract Chol/lipid into mixed micelles in the aqueous phase [26]. However, digitonin does not elicit drastic chain disordering, as seen in the DPH anisotropy results. This result may suggest that the saponin acts on a limited portion of the membrane rather than destabilizing the entire membrane, thus largely preserving the lamellar structure of the POPC and POPC–sterol membranes (Figs. S4, S7, and S8). This observation was in parallel with previous reports [42][45].

In this study, we focused on the importance of the size of saponin’s sugar chain, particularly its interaction with membrane lipids and Chol. One sugar unit attached to the sapogenin, diosgenin, was not enough to cause significant membrane-disrupting effects. The prominent differences between TRL and DSN imply that

the sugar moiety must be of considerable size to evoke damage to the bilayer integrity and efficiently elicit the saponin/Chol/phospholipid complexes.

Table 1. Summary of NMR data for Chol, diosgenin, TRL, DSN, and digitonin in POPC bilayers

^{2}H/^{31}P-observed sterol or lipid	Sterol in bilayers (10 mol%)	Sterol and Saponin in POPC (10 mol%)					
		Non	Chol	diosgenin	TRL	DSN	Digitonin
^{2}H Δν of 3*d*-Chol (kHz)	Chol		43.8[b,c]	42.0[b,d]	41.0	38.7	-
^{2}H Δν of 3*d*-diosgenin (kHz)	diosgenin[e]		42.1[b,d]	41.1[b,c]	41.1	38.9	-
^{2}H $\Delta\nu$ of 10′,10′d_2-POPC (kHz)	Not added	19		23[b]	23	21	19[g]
	Chol		25[b]	-	30	23	20[g]
^{31}P CSA ($\delta_{//} - \delta\perp$) of POPC (ppm)	Not added	45.9[f]	-	45.1	45.5	47.1	44.9
	Chol		45.4	44.5	45.5	40.1	44.1
	diosgenin[e]			45.1	45.5	44.5	44.3

[a]Data obtained from pure MLVs of POPC. [b]Derived from a previous study [14]. [c]3*d*-Chol or 3*d*-diosgenin concentration was 10 mol%, and non-labeled sterol was added. [d]3*d*-Chol and diosgenin or Chol and 3*d*-diosgenin concentrations were 9 mol% (total sterol 18 mol%). [e]Additional results of diosgenin-containing bilayers are provided in Table S1 and Figs. S4, S9, and S9. [f]The average value was measured in this study under the same conditions, which was consistent with the reported values for ^{31}P CSA of POPC in bilayers [45][46]. [g]In the presence of digitonin, the ^{2}H signals of POPC-based MLVs were significantly attenuated (see Fig. S7).

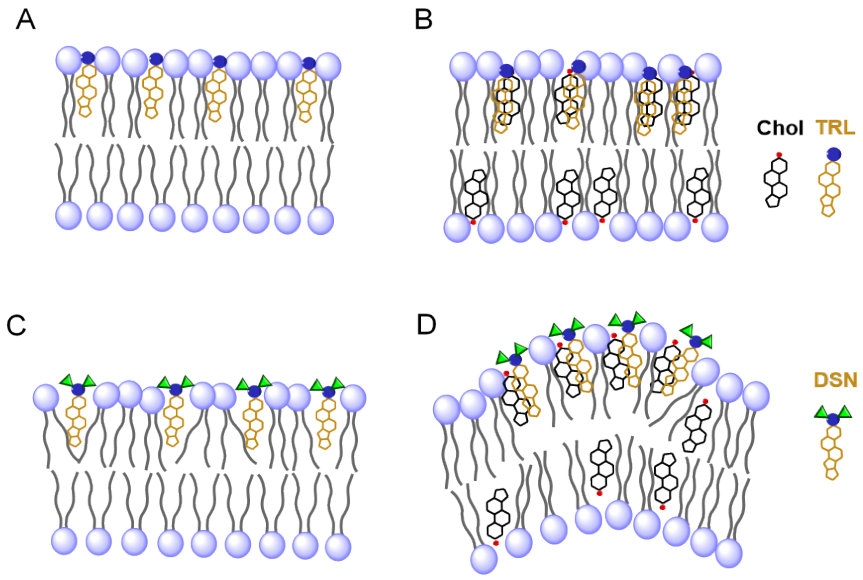

Figure 8. Schematic illustration of diosgenyl saponins' interaction with the interior of an outer layer of membranes. TRL (trillin, Panels **A** and **B**) and DSN (dioscin, Panels **C** and **D**) in PC membranes (Panels A and C without Chol and Panels B and D with Chol). The curved bilayers in Panel D are illustrated based on the report of Frenkel et al. [26]. Even in the absence of Chol, DSN can be incorporated into bilayers (C). There may be a considerable amount of TRL and DSN staying on the surface of the bilayers, which are not illustrated in the panels.

5. Conclusion

We established the modalities of the membrane activities of diosgenyl saponins: the number of sugars dictates the extent of membrane disruption. The diosgenin backbone, which has a flat, hydrophobic structure similar to that of Chol, assimilated into the phospholipid bilayer and therefore increases the chances of interaction with membrane receptors and signaling platforms or incorporation into the cell, resulting in the exertion of their strong biological activities. The bioactivities of TRL, which show no hemolytic potential, may be mediated by this mechanism. The low hemolytic toxicity of this saponin is particularly preferable, as this benign behavior can be manipulated for further pharmacological studies. Regarding DSN and its multifaceted pharmacological activities, its strong membrane interaction is influenced not only by this mechanism but also by its association with membrane lipids such as Chol and phospholipids.

Funding

The study was supported in part by KAKENHI Grant Numbers, 19K0513 (S.H.) and 21H04707 (M.M) from the Japan Society for the Promotion of Science (JSPS).

CRediT authorship contribution statement

J.C.O., S. H. and M.M. designed the research. J.C.O. largely performed the experiments in the present study. D.G.M. and Y. U. performed some of the fluorescence experiments and ^{31}P NMR measurements. A. M. prepared ^{2}H-labeled phospholipids. All the authors analyzed the obtained data. J.C.O., S. H. and M.M. contributed to article writing. All authors approved the final version of the manuscript.

Declaration of competing interest

The authors declare that they have no known competing financial interests or personal relationships that could have appeared to influence the work reported in this paper.

Acknowledgements

We are grateful to Profs. J. P. Slotte, Åbo Akademi University for helpful discussions. We thank Drs. Y. Todokoro and N. Inazumi, Osaka University for their technical help in solid-state NMR measurements.

Appendix A. Supporting Data

Supplementary data for this article can be found online at xxx.

References

[1] M. Marrelli, F. Conforti, F. Araniti, G.A. Statti, Effects of Saponins on Lipid Metabolism: A Review of Potential Health Benefits in the Treatment of Obesity, Molecules. 21 (2016). https://doi.org/10.3390/molecules21101404.

[2] A. Osbourn, Saponins and plant defence — a soap story, Trends in Plant Science. 1 (1996) 4–9. https://doi.org/https://doi.org/10.1016/S1360-1385(96)80016-1.

[3] X. Zhang, M. Jin, N. Tadesse, J. Dang, T. Zhou, H. Zhang, S. Wang, Z. Guo, Y. Ito, Dioscorea zingiberensis C. H. Wright: An overview on its traditional use, phytochemistry, pharmacology, clinical applications, quality control, and toxicity, Journal of Ethnopharmacology. 220 (2018) 283–293. https://doi.org/10.1016/j.jep.2018.03.017.

[4] T. Chen, W. Jiang, H. Zhang, X. You, M. Liu, L. Wang, P. Xiang, L. Xu, D. Zheng, X. Zhang, H. Ji, K. Hao, T. Yan, Protective effect of trillin against ethanol-induced acute gastric lesions in an animal model, (2016). https://doi.org/10.1039/c5ra21158a.

[5] W. Jiang, F. Luo, Q. Lu, J. Liu, P. Li, X. Wang, Y. Fu, K. Hao, T. Yan, X. Ding, The protective effect of Trillin LPS-induced acute lung injury by the regulations of inflammation and oxidative state, Chemico-Biological Interactions. 243 (2016) 127–134. https://doi.org/https://doi.org/10.1016/j.cbi.2015.09.010.

[6] X. Tao, L. Yin, L. Xu, J. Peng, Dioscin: A diverse acting natural compound with therapeutic potential in metabolic diseases, cancer, inflammation and infections, Pharmacological Research. 137 (2018) 259–269. https://doi.org/10.1016/j.phrs.2018.09.022.

[7] M. Tang, C. Taghibiglou, The Mechanisms of Action of Curcumin in Alzheimer's Disease, Journal of Alzheimer's Disease. 58 (2017) 1003–1016. https://doi.org/10.3233/JAD-170188.

[8] M. Nishikawa, S. Nojima, T. Akiyama, U. Sankawa, K. INOUE, Interaction of Digitonin and Its Analogs with Membrane Cholesterol1, The Journal of Biochemistry. 96 (1984) 1231–1239. https://doi.org/10.1093/oxfordjournals.jbchem.a134941.

[9] G. Francis, Z. Kerem, H.P.S. Makkar, K. Becker, The biological action of saponins in animal systems: a review, British Journal of Nutrition. 88 (2002) 587–605. https://doi.org/10.1079/BJN2002725.

[10] Ö. Güçlü-Üstündağ, G. Mazza, Saponins: Properties, Applications and Processing, Critical Reviews in Food Science and Nutrition. 47 (2007) 231–258. https://doi.org/10.1080/10408390600698197.

[11] M.H.K. Konoki, K. Tachibana, Cholesterol-independent membrane disruption caused by triterpenoid saponins, Biochimica et Biophysica Acta - Lipids and Lipid Metabolism. 1299 (1996) 252–258. https://doi.org/10.1016/0005-2760(95)00214-6.

[12] Y. Ohnishi, K. Tachibana, Synthesis of pavoninin-1, a shark repellent substance, and its structural analogues toward mechanistic studies on their membrane perturbation, Bioorganic and Medicinal Chemistry. (1997). https://doi.org/10.1016/S0968-0896(97)00170-3.

[13] S.L. Verstraeten, M. Deleu, M. Janikowska-Sagan, E.J.S. Claereboudt, L. Lins, D. Tyteca, M.P. Mingeot-Leclercq, The activity of the saponin ginsenoside Rh2 is enhanced by the interaction with membrane sphingomyelin but depressed by cholesterol, Scientific Reports. 9 (2019) 1–14. https://doi.org/10.1038/s41598-019-43674-w.

[14] J.C. Ondevilla, S. Hanashima, A. Mukogawa, Y. Umegawa, M. Murata, Diosgenin-induced physicochemical effects on phospholipid bilayers in comparison with cholesterol, Bioorganic and Medicinal Chemistry Letters. 36 (2021). https://doi.org/10.1016/j.bmcl.2021.127816.

[15] T. Xia, Y.N. Wang, C.X. Zhou, L.M. Wu, Y. Liu, Q.H. Zeng, X.L. Zhang, J.H. Yao, M. Wang, J.P. Fang, Ginsenoside Rh2 and Rg3 inhibit cell proliferation and induce apoptosis by increasing mitochondrial reactive oxygen species in human leukemia Jurkat cells, Molecular Medicine Reports. 15 (2017) 3591–3598. https://doi.org/10.3892/mmr.2017.6459.

[16] C. De Groot, C.C. Müller-Goymann, Saponin Interactions with Model Membrane Systems - Langmuir Monolayer Studies, Hemolysis and Formation of ISCOMs, Planta Medica. 82 (2016) 1496–1512. https://doi.org/10.1055/s-0042-118387.

[17] S.L. Verstraeten, J.H. Lorent, M.P. Mingeot-Leclercq, Lipid Membranes as Key Targets for the Pharmacological Actions of Ginsenosides, Frontiers in Pharmacology. 11 (2020) 1–13. https://doi.org/10.3389/fphar.2020.576887.

[18] A. Watts, Solid-state NMR in drug design and discovery for membrane-embedded targets, Nature Reviews Drug Discovery. 4 (2005) 555–568. https://doi.org/10.1038/nrd1773.

[19] R. Mani, S.D. Cady, M. Tang, A.J. Waring, R.I. Lehrer, M. Hong, Membrane-dependent oligomeric structure and pore formation of a beta-hairpin antimicrobial peptide in lipid bilayers from solid-state NMR., Proceedings of the National Academy of Sciences of the United States of America. 103 (2006) 16242–16247. https://doi.org/10.1073/pnas.0605079103.

[20] S. Matsuoka, M. Murata, Cholesterol markedly reduces ion permeability induced by membrane-bound amphotericin B, Biochimica et Biophysica Acta - Biomembranes. (2002). https://doi.org/10.1016/S0005-2736(02)00491-1.

[21] Y. Umegawa, T. Yamamoto, M. Dixit, K. Funahashi, S. Seo, Y. Nakagawa, T. Suzuki, S. Matsuoka, H. Tsuchikawa, S. Hanashima, T. Oishi, N. Matsumori, W. Shinoda, M. Murata, Amphotericin B assembles into seven-molecule ion channels: An NMR and molecular dynamics study, Science Advances. 8 (2022) 1–11. https://doi.org/10.1126/sciadv.abo2658.

[22] S. Matsuoka, M. Murata, Membrane permeabilizing activity of amphotericin B is affected by chain length of phosphatidylcholine added as minor constituent, Biochimica et Biophysica Acta - Biomembranes. (2003). https://doi.org/10.1016/j.bbamem.2003.09.010.

[23] T. Yasuda, M. Kinoshita, M. Murata, N. Matsumori, Detailed comparison of deuterium quadrupole profiles between sphingomyelin and phosphatidylcholine bilayers, Biophysical Journal. 106 (2014) 631–638. https://doi.org/10.1016/j.bpj.2013.12.034.

[24] T. Yasuda, H. Tsuchikawa, M. Murata, N. Matsumori, Deuterium NMR of Raft Model Membranes Reveals Domain-Specific Order Profiles and Compositional Distribution, Biophysical Journal. (2015). https://doi.org/10.1016/j.bpj.2015.04.008.

[25] S. Hanashima, Y. Ibata, H. Watanabe, T. Yasuda, H. Tsuchikawa, M. Murata, Side-chain deuterated cholesterol as a molecular probe to determine membrane order and cholesterol partitioning, Organic and Biomolecular Chemistry. 17 (2019). https://doi.org/10.1039/c9ob01342c.

[26] N. Frenkel, A. Makky, I.R. Sudji, M. Wink, M. Tanaka, Mechanistic investigation of interactions between steroidal saponin digitonin and cell membrane models, Journal of Physical Chemistry B. 118 (2014) 14632–14639. https://doi.org/10.1021/jp5074939.

[27] V.L. Challinor, J.J. De Voss, Open-chain steroidal glycosides, a diverse class of plant saponins, Natural Product Reports. 30 (2013) 429–454. https://doi.org/10.1039/c3np20105h.

[28] O. Engberg, H.A. Scheidt, T.K.M. Nyholm, J.P. Slotte, D. Huster, Membrane Localization and Lipid Interactions of Common Lipid-Conjugated Fluorescence Probes, Langmuir. 35 (2019) 11902–11911. https://doi.org/10.1021/acs.langmuir.9b01202.

[29] R. Malabed, S. Hanashima, M. Murata, K. Sakurai, Sterol-recognition ability and membrane-disrupting activity of Ornithogalum saponin OSW-1 and usual 3-O-glycosyl saponins, Biochimica et Biophysica Acta - Biomembranes. 1859 (2017). https://doi.org/10.1016/j.bbamem.2017.09.019.

[30] T. Parasassi, G. De Stasio, G. Ravagnan, R.M. Rusch, E. Gratton, Quantitation of lipid phases in phospholipid vesicles by the generalized polarization of Laurdan fluorescence, Biophysical Journal. 60 (1991) 179–189. https://doi.org/10.1016/S0006-3495(91)82041-0.

[31] R. Malabed, S. Hanashima, M. Murata, K. Sakurai, Interactions of OSW-1 with Lipid Bilayers in Comparison with Digitonin and Soyasaponin, Langmuir. 36 (n.d.) 3600–3610. https://doi.org/10.1021/acs.langmuir.9b03957.

[32] W. Li, Z. Qiu, Y. Wang, Y. Zhang, M. Li, J. Yu, L. Zhang, Z. Zhu, B. Yu, Synthesis, cytotoxicity, and hemolytic activity of 6′-O-substituted dioscin derivatives, Carbohydrate Research. 342 (2007) 2705–2715. https://doi.org/10.1016/j.carres.2007.09.004.

[33] P. Jurkiewicz, L. Cwiklik, P. Jungwirth, M. Hof, Lipid hydration and mobility: An interplay between fluorescence solvent relaxation experiments and molecular dynamics simulations, Biochimie. 94 (2012) 26–32. https://doi.org/10.1016/j.biochi.2011.06.027.

[34] T. Parasassi, E.K. Krasnowska, L. Bagatolli, E. Gratton, Laurdan and Prodan as Polarity-Sensitive Fluorescent Membrane Probes, Journal of Fluorescence,. 8 (1998) 365–373.

[35] N. Matsumori, T. Yasuda, H. Okazaki, T. Suzuki, T. Yamaguchi, H. Tsuchikawa, M. Doi, T. Oishi, M. Murata, Comprehensive Molecular Motion Capture for Sphingomyelin by Site-Specific Deuterium Labeling, Biochemistry. 51 (2012) 8363–8370. https://doi.org/10.1021/bi3009399.

[36] S. Hanashima, N. Fukuda, R. Malabed, M. Murata, M. Kinoshita, P. Greimel, Y. Hirabayashi, β-Glucosylation of cholesterol reduces sterol-sphingomyelin interactions, Biochimica et Biophysica Acta - Biomembranes. 1863 (2021) 183496. https://doi.org/10.1016/j.bbamem.2020.183496.

[37] K. Bin Kang, J. Ryu, Y. Cho, S.-Z. Choi, M. Son, S.H. Sung, Combined Application of UHPLC-QTOF/MS, HPLC-ELSD and 1 H-NMR Spectroscopy for Quality Assessment of DA-9801, A Standardised Dioscorea Extract, Phytochemical Analysis. 28 (2017) 185–194. https://doi.org/10.1002/pca.2659.

[38] H.A. Scheidt, P. Müller, A. Herrmann, D. Huster, The Potential of Fluorescent and Spin-labeled Steroid Analogs to Mimic Natural Cholesterol, Journal of Biological Chemistry. 278 (2003) 45563–45569. https://doi.org/10.1074/jbc.M303567200.

[39] H.A. Scheidt, T. Meyer, J. Nikolaus, D.J. Baek, I. Haralampiev, L. Thomas, R. Bittman, P. Müller, A. Herrmann, D. Huster, Cholesterol's aliphatic side chain modulates membrane properties, Angewandte Chemie - International Edition. 52 (2013) 12848–12851. https://doi.org/10.1002/anie.201306753.

[40] J.R. Robalo, J.P.P. Ramalho, D. Huster, L.M.S. Loura, Influence of the sterol aliphatic side chain on membrane properties: A molecular dynamics study, Physical Chemistry Chemical Physics. 17 (2015) 22736–22748. https://doi.org/10.1039/c5cp03097h.

[41] R. Malabed, S. Hanashima, M. Murata, K. Sakurai, Sterol-recognition ability and membrane-disrupting activity of Ornithogalum saponin OSW-1 and usual 3-O-glycosyl saponins, BBA - Biomembranes. 1859 (2017) 2516–2525. https://doi.org/10.1016/j.bbamem.2017.09.019.

[42] M. Nazari, M. Kurdi, H. Heerklotz, Classifying surfactants with respect to their effect on lipid membrane order, Biophysical Journal. 102 (2012) 498–506. https://doi.org/10.1016/j.bpj.2011.12.029.

[43] M. Kinoshita, K.G. Suzuki, N. Matsumori, M. Takada, H. Ano, K. Morigaki, M. Abe, A. Makino, T. Kobayashi, K.M. Hirosawa, T.K. Fujiwara, A. Kusumi, M. Murata, Raft-based sphingomyelin interactions revealed by new fluorescent sphingomyelin analogs, The Journal of Cell Biology. 216 (2017). https://doi.org/10.1083/jcb.201607086.

[44] D.L. Garza, S. Hanashima, Y. Umegawa, M. Murata, M. Kinoshita, N. Matsumori, P. Greimel, Behavior of Triterpenoid Saponin Ginsenoside Rh2 in Ordered and Disordered Phases in Model Membranes Consisting of Sphingomyelin, Phosphatidylcholine, and Cholesterol, Langmuir. 38 (2022) 10478–10491. https://doi.org/10.1021/acs.langmuir.2c01261.

[45] T. Akiyama, S. Takagi, U. Sankawa, S. Inari, H. Saitô, Saponin-Cholesterol Interaction in the Multibilayers of Egg Yolk Lecithin As Studied by Deuterium Nuclear Magnetic Resonance: Digitonin and Its Analogues, Biochemistry. 19 (1980) 1904–1911. https://doi.org/10.1021/bi00550a027.

[46] P.R. Cullis, B. De Kruyff, R.E. Richards, Factors affecting the motion of the polar headgroup in phospholipid bilayers. A 31P NMR study of unsonicated phosphatidylcholine liposomes., Biochimica et Biophysica Acta. 426 (1976) 433–446. https://doi.org/10.1016/0005-2736(76)90388-6.